

Electronic Supplementary Information (ESI)

Ti-MOF Single-Crystals Featuring Intracrystal Macro-Microporous Hierarchy for Catalytic Oxidative Desulfurization

Shen Yu,^{ab} Yu Xiao,^a Zhan Liu,^{abc} Jia-Min Lyu,^a Yi-Long Wang,^d Zhi-Yi Hu,^{ac} Yu Li,^a Ming-Hui Sun,^e Li-Hua Chen^{*a} and Bao-Lian Su^{*ac}

* To whom correspondence should be addressed: Li-Hua Chen (chenlihua@whut.edu.cn); Bao-Lian Su (bao-lian.su@unamur.be)

^a Laboratory of Living Materials at the State Key Laboratory of Advanced Technology for Materials Synthesis and Processing, Wuhan University of Technology, 122 Luoshi Road, Wuhan, 430070, Hubei, China

^b International School of Materials Science and Engineering, Wuhan University of Technology, Wuhan, 430070, Hubei, China

^c Nanostructure Research Center, Wuhan University of Technology, Wuhan, 430070, Hubei, China

^d School of Chemistry, Chemical Engineering and Life Science, Wuhan University of Technology, Wuhan, 430070, Hubei, China

^e Laboratory of Inorganic Materials Chemistry, University of Namur, 61 rue de Bruxelles, B-5000 Namur, Belgium

Experimental section

Chemicals

All the chemicals were commercially purchased and used without any further treatment. Styrene (> 99.5%), NaOH (> 96%), potassium persulfate (> 99.5%), ethanol (> 99.7%), trichloromethane (> 99%), and tert-butylhydroperoxide (> 65 wt%) were bought from Sinopharm Chemical Reagent Co., Ltd. 2,5-Dihydroxyterephthalic acid (> 98%), isopropanol (> 99.5%), acetonitrile (> 99.5%), N,N-Dimethylformamide (> 99.5%), benzothiophene (> 97%), dibenzothiophene (> 99%), 4,6-dimethyldibenzothiophene (> 97%), decane (> 99.5%), dodecane (> 99.5%), and n-octane (> 96%) were purchased from Aladdin. Titanium isopropoxide (> 95%) was from Macklin.

Synthesis of polystyrene (PS) spheres

Previous literatures indicate that PS spheres with a diameter of 400-500 nm are better templates for self-assembly process compared to other diameters.^{1,2} Therefore, PS spheres with a diameter of ~ 490 nm were synthesized by a soap-free polymerization method.² Firstly, raw styrene was treated with a NaOH solution (2 M in water) by vigorous stirring for 30 min. Then, 47 g of the dealt styrene was added into 400 g of deionized H₂O. The mixture was kept in a three-neck flask under stirring (600 rpm) and a N₂ atmosphere. Hereafter, the temperature of the system was elevated to 80°C, followed by the addition of 0.43 g of potassium persulfate to trigger the polymerization reaction. The reaction was further performed at 80°C for 5 h under stirring (600 rpm) and a N₂ atmosphere. Finally, a powder of PS spheres was obtained by drying the solution under 60°C for 24 h. The PS powder was finely ground for further use.

Preparation of the conventional microporous NTU-9 single-crystals

The conventional microporous NTU-9 single-crystals (C-NTU-9) were synthesized by a modified method according to a previous method reported by another literature.³ Firstly, 204 mg (1.03 mmol) of 2,5-dihydroxyterephthalic acid (DODBC) was added into a mixture of 4 mL of isopropanol and 4 mL of acetonitrile. The brown mixture was kept stirring vigorously for 1 h. Hereafter, 75 μL of titanium isopropoxide (TIP) was added quickly into the above solution to form an orange slurry. The orange slurry was kept stirring vigorously for another 1 h and transformed into a Teflon-lining. The lining was sealed by a stainless-autoclave and put under 100-120°C for 24 h. Finally, the wine-red product was collected by filtering, washing with ethanol thoroughly, and drying at 60°C.

Preparation of hierarchically macro-microporous NTU-9 single-crystals

A novel vapor-assisted polymer-templated method was used to synthesize the hierarchically macro-microporous NTU-9 single-crystals. Firstly, different amounts of the as-prepared PS powder (0.5, 1.0, or 1.5 g) and 0.204 g of DODBC were added into 10 mL of isopropanol and the mixture was kept stirring vigorously for 1 h and kept under ultrasonic treatment for another 1 h. Hereafter, 75 μ L of titanium isopropoxide (TIP) was added quickly into the above mixture to form an orange slurry and the slurry was kept stirring vigorously for 1 h and kept under ultrasonic treatment for another 1 h. The homogeneous slurry was poured into a watch glass and kept under 40°C for 4 h and subsequently 80°C for 2 h to achieve a self-assembly process. The resultant composite fragments were placed into the upper part of a Teflon-lining with a mixed solution of 10 mL of isopropanol and 10 mL of acetonitrile underneath. The equipment was sealed by a stainless-autoclave and put under 100-120°C for 12-72 h. The product was obtained and immersed into 50 mL of N,N-Dimethylformamide (DMF) for 4 h to remove the PS templates. Finally, the hierarchically macro-microporous NTU-9 single-crystals (denoted as Hier-NTU-9-S1, Hier-NTU-9-S2, and S3 according to the amount of PS template to be 0.5 g, 1.0 g, and 1.5 g, respectively) were obtained by filtering, washing with ethanol thoroughly, and drying at 60°C.

Exchange and removal of organic solvents

A solvent exchange process is important to remove the residual isopropanol, acetonitrile, and DMF.³ All as-obtained NTU-9 samples were mixed with 20 mL of trichloromethane and kept stirring (200 rpm) for 48 h. The final products were obtained by filtering, washing with trichloromethane thoroughly, and drying at 160°C.

Catalyst characterizations

Power X-radiation diffraction (XRD) patterns were recorded on a D8 ADVANCE with Cu K α radiation ($\lambda = 1.5413 \text{ \AA}$) at a tube voltage of 40 kV and a tube current of 40 mA under ambient conditions. Data was collected at 2θ ranging from 5° to 60° with a step of 0.05°/min.

The scanning electron microscopy (SEM) was collected on a Hitachi S-4800 scanning electron microscopy with extraction voltage of 5.0 kV and acceleration current of 10.0 μ A. SEM was equipped with Energy Dispersive X-Ray Spectroscopy (EDS) for the elemental analysis and mapping.

Infrared (IR) spectrum was recorded on a Bruker Vertex 80v Fourier transform infrared (FT-IR) spectrometer in a vacuum atmosphere at room temperature using a KBr wafer technique. Scanning range: 4000–400 cm^{-1} ; scan times: 64; vacuum degree: < 5 hPa.

Thermogravimetric analysis-differential scanning calorimetry (TG-DSC) was conducted in air (20 mL/min) on Labsys Evo. A ramp of 10°C/min was used from room temperature to 800°C.

N₂ adsorption-desorption isotherms were recorded using a Micromeritics ASAP 3020 gas sorptiometer after the samples were degassed at 160°C under vacuum for 8 h. The micropore and external surface area were determined from N₂ adsorption using the Brunauer-Emmett-Teller method. Micropore size was calculated by a Horvath-Kawazoe method. Using the Barret-Joyner-Halenda model, mesopore volume and mesopore size were determined by the desorption branches of N₂ isotherms. Total pore volumes were estimated from the adsorbed amount at a relative pressure P/P_0 of 0.99.

Mercury intrusion porosimetry (MIP) was performed with a Micromeritics Autopore IV 9500 operated in the pressure range from vacuum to 207 MPa. Samples were degassed in situ prior to measurement. The pore size distribution was determined by application of the Washburn equation.

Water contact angle test was conducted on dataphysics OCA 35 equipped with a digital camera. The water droplet was controlled to be 2 μL for each test.

A Lambda 750 S equipment was applied to obtain Ultraviolet-visible (UV-vis) diffuse reflectance spectrum in the wavelength ranging from 800 nm to 200 nm with BaSO₄ as the reference sample.

X-ray photoelectron spectroscopy (XPS) was performed on Thermo Scientific K-Alpha+ (Thermo Fisher) spectrometer equipped with a mono Al-Kα X-ray source (excitation energy = 1486.6 eV). Spectrum curve fitting was carried out by using the XPSPEAK41 software.

Catalytic tests

Oxidative desulfurization (ODS): A certain amount of benzothiophene (BT), dibenzothiophene (DBT), or 4,6- dimethyldibenzothiophene (DMDBT) was dissolved in n-octane to act as a model fuel (decane or dodecane were used as internal standards). The concentration of sulfur in each model fuel was 1000, 1000, and 500 ppm for BT, DBT, and 4,6-DMDBT, respectively. The reaction was performed in a 25 mL two-neck glass flask in an oil bath under vigorous stirring (600 rpm). In a typical run, 5 mL of model fuel and 20 mg of catalyst were added to the flask. Then, the temperature of the mixture was raised to 80°C (a common reaction temperature when using Ti-MOFs as catalysts) and kept to be stable. Tert-butylhydroperoxide (TBHP) was used as an oxidant and the molar ratio of TBHP to sulfur in model fuel was 4. That is 31, 23, and 10 μL of TBHP for the ODS of BT, DBT, and 4,6-DMDBT. After adding TBHP into the mixture, the reaction was triggered and kept for a certain time. A small aliquots (~200 μL) of the reaction solution were extracted as a function of time

through a 0.22 μm syringe filter (to remove suspended catalyst and stop the reactions from proceeding). All the organic components were determined quantitatively by a gas chromatography (GC 7890B) equipped with a flame-ionization detector. The reactant conversion (X) is calculated by **Equation (1)** as following:

$$X = \left(1 - \frac{\frac{A_R}{A_I}}{\frac{A_{R0}}{A_{I0}}}\right) \times 100\% \quad \text{Equation (1)}$$

A_R , A_I , A_{R0} , and A_{I0} represents the peak area of reactant, internal standard, initial reactant, initial internal standard determined by GC, respectively.

Recyclability. Catalysts were collected after every reaction cycle from reaction solutions, washed and dried at 120°C for overnight. The obtained catalysts (recovery ratio > 95 wt% for every time) were reused in the next reaction cycle with the same ratio of reactant mixture: TBHP: catalyst: organic solvent: model fuel as the 1st cycle.

Supporting Figures and Tables

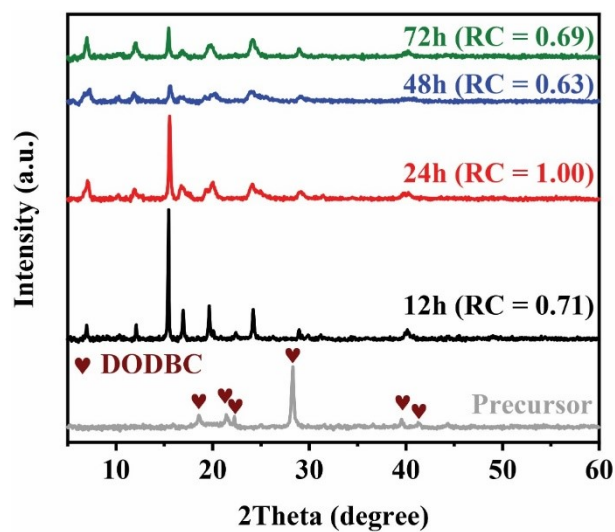


Fig. S1 XRD patterns of samples at different stages during a “crystallization-dissolution-recrystallization” procedure using our novel vapor-assisted polymer-templated method. The relative crystallinity (RC) is labeled.

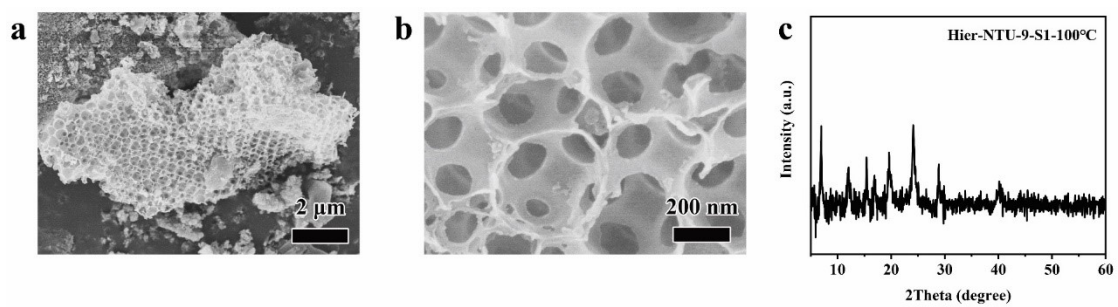


Fig. S2 (a, b) SEM images and (c) XRD pattern of a sample obtained under 100°C rather than 120°C using our novel vapor-assisted polymer-templated method.

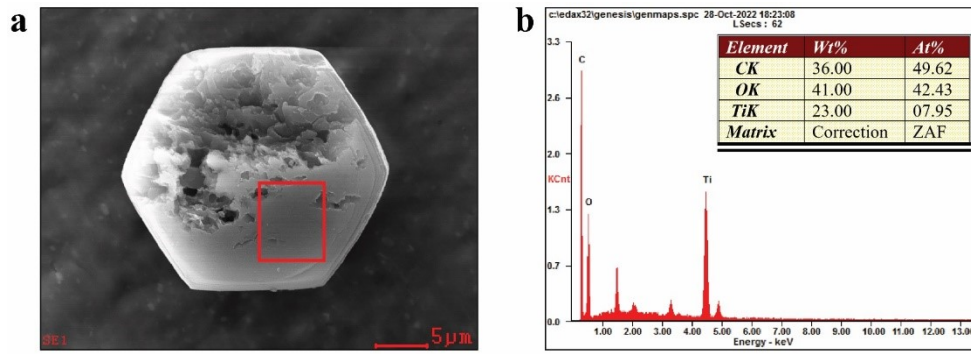


Fig. S3 Elemental analysis of a hierarchically macro-microporous NTU-9 sing-crystal (Hier-NTU-9-S1). (a) a SEM image showing the crystal morphology and the detection area (red square) and (b) elemental composition analysis.

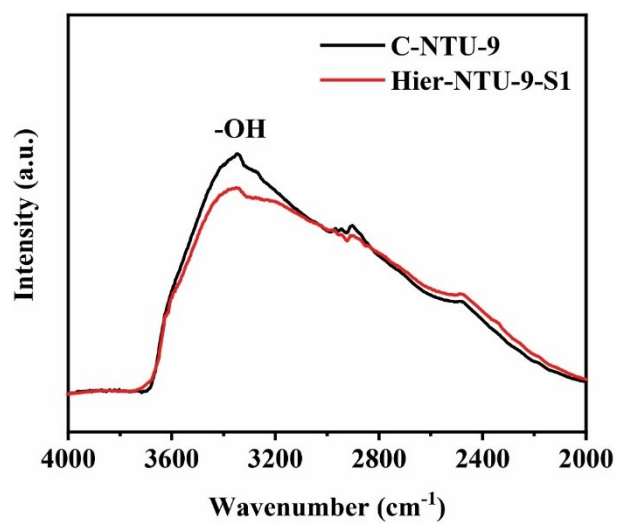


Fig. S4 IR spectra ranging from 2000-4000 cm⁻¹ of the hierarchically macro-microporous NTU-9 single-crystal (Hier-NTU-9-S1) and the conventional NTU-9 (C-NTU-9).

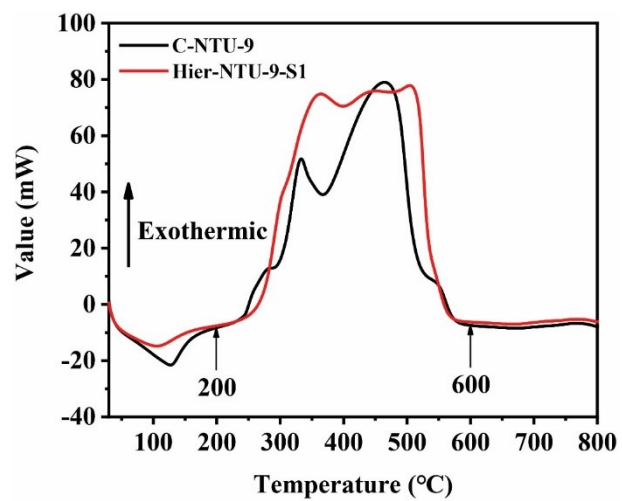


Fig. S5 DSC curves of the hierarchically macro-microporous NTU-9 single-crystal (Hier-NTU-9-S1) and the conventional NTU-9 (C-NTU-9).

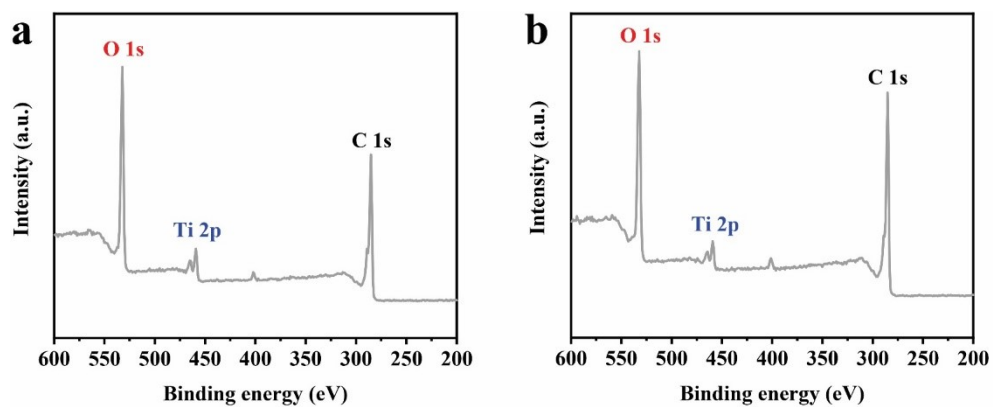


Fig. S6 XPS results of (a) the hierarchically macro-microporous NTU-9 single-crystal (Hier-NTU-9-S1) and (b) the conventional NTU-9 (C-NTU-9).

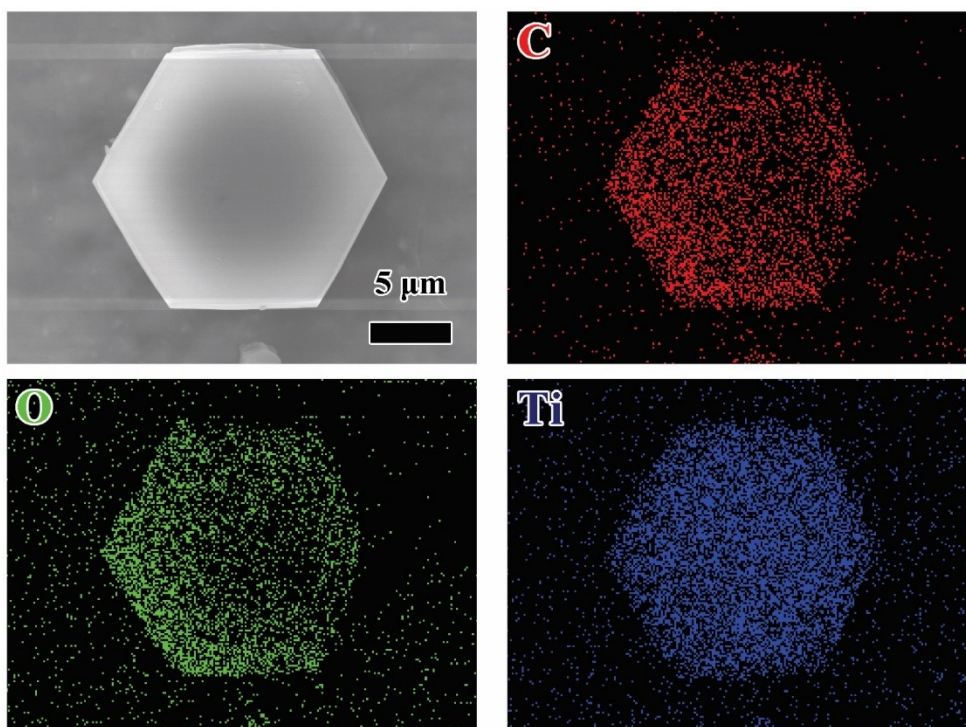


Fig. S7 EDS mappings of the conventional NTU-9 (C-NTU-9).

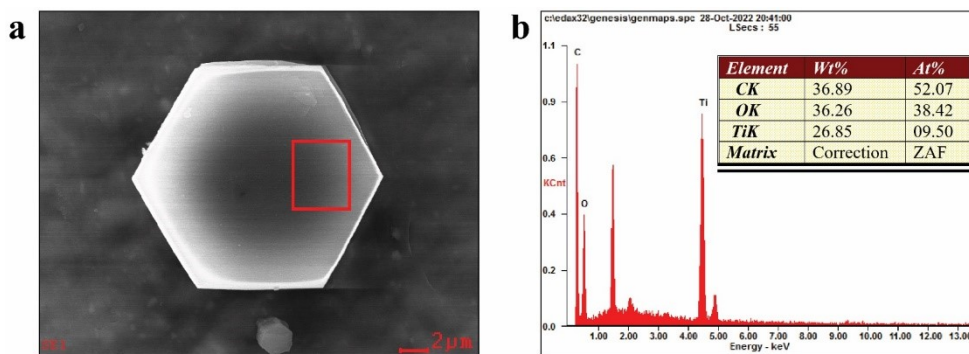


Fig. S8 Elemental analysis of the conventional NTU-9 (C-NTU-9). (a) a SEM image showing the crystal morphology and the detection area (red square) and (b) elemental composition analysis.

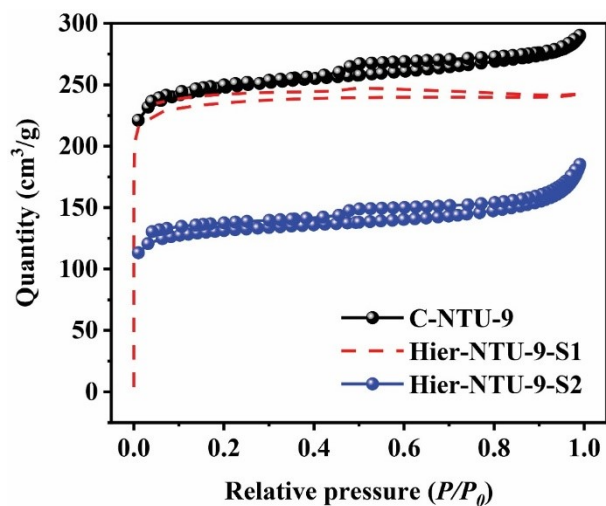


Fig. S9 N₂ adsorption-desorption isotherms of different samples.

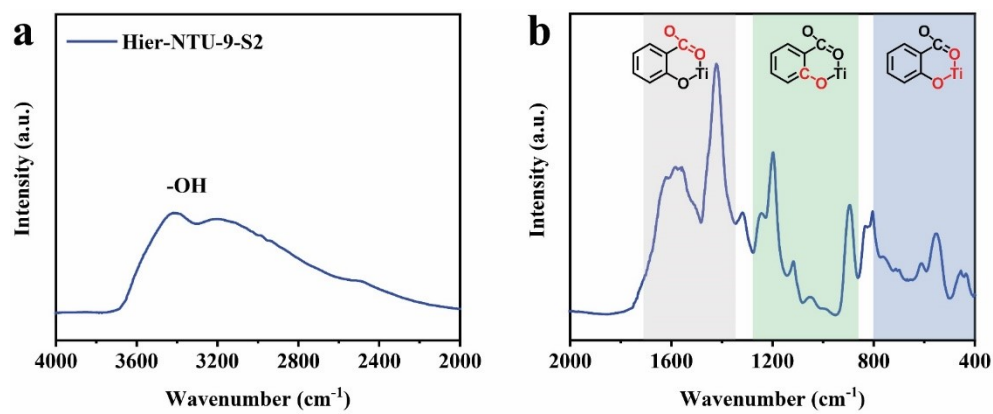


Fig. S10 IR spectrum of another hierarchically macro-microporous NTU-9 sing-crystal (Hier-NTU-9-S2) ranging from (a) 2000-4000 cm^{-1} or (b) 400-2000 cm^{-1} .

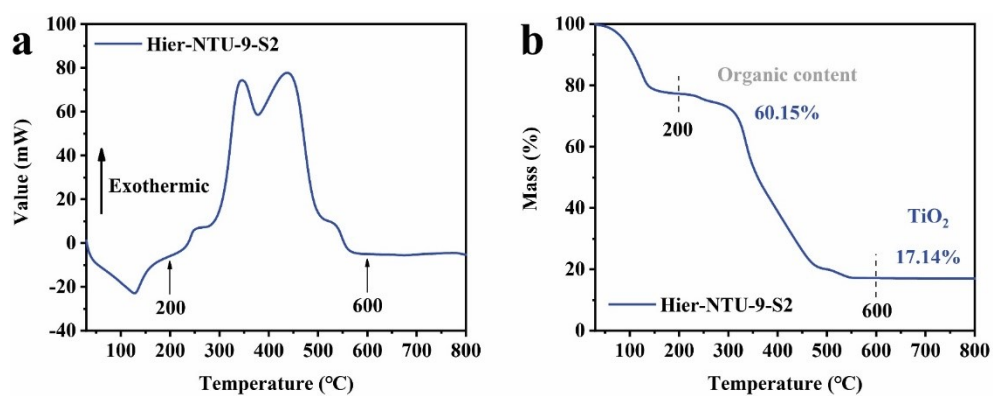


Fig. S11 (a) DSC curve and (b) TG curve of another hierarchically macro-microporous NTU-

9 sing-crystal (Hier-NTU-9-S2).

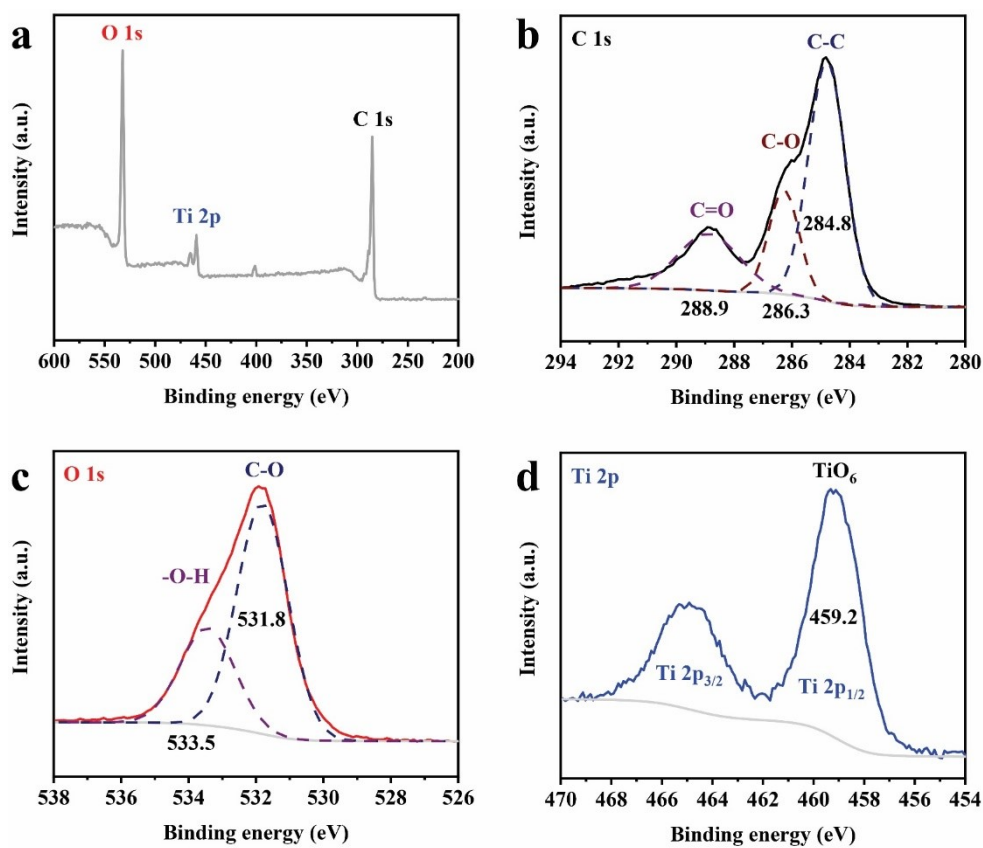


Fig. S12 (a-d) XPS results of another hierarchically macro-microporous NTU-9 sing-crystal (Hier-NTU-9-S2)

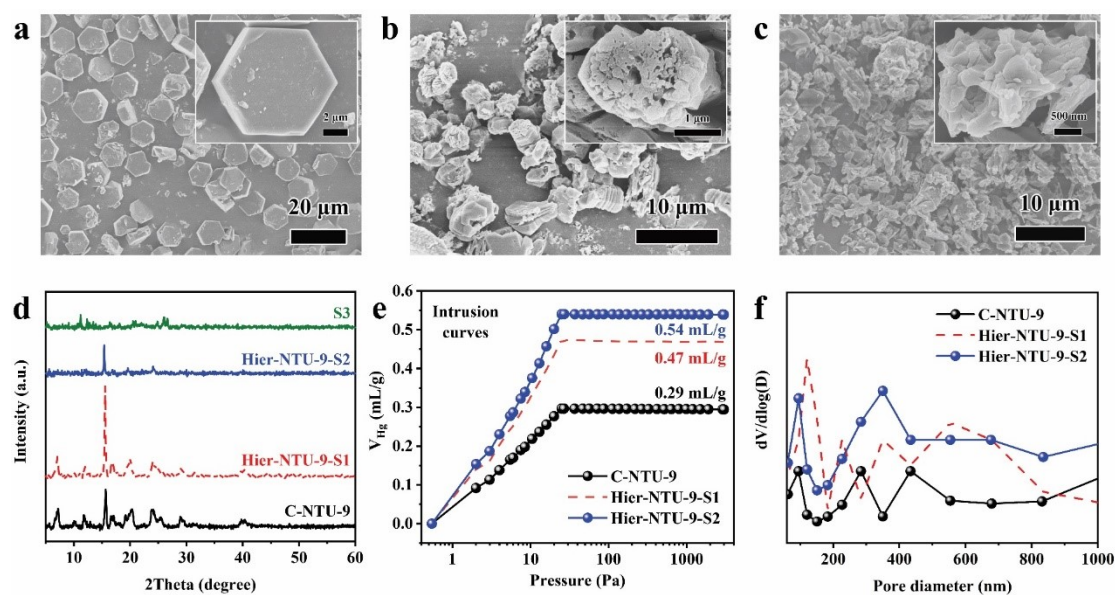


Fig. S13 Investigations of the effect of polymer templates on the macroporous structure of the Hier-NTU-9. (a-c) SEM images of C-NTU-9 (0 g of PS), Hier-NTU-9-S2 (1.0 g of PS), and S3 (1.5 g of PS), respectively. (d) XRD patterns of corresponding samples. (e) Mercury intrusion curve and (the inset) macropore size distribution of corresponding samples.

As shown in **Figure S7-9** and **Figure S13**, the conventional C-NTU-9 possesses a typical hexagonal morphology with a crystal size of $\sim 10 \mu\text{m}$, and the crystal surface is intact with no any secondary pore. When a novel vapor-assisted polymer-templated method was used, 0.5 g of PS template produced a Hier-NTU-9-S1 as mentioned above. As the content of PS template further increased to 1.0 g (Hier-NTU-9-S2 in **Figure S9-12** and **Figure S13**), the crystal evolved into an irregular morphology with macropores ($< 500 \text{ nm}$) and a much lower crystallinity was obtained, which indicated that excessive PS templates hindered the crystal growth by preventing the contacting between the solvent vapors and the precursor. This hypothesis is further evidenced by the phenomenon that a sample S3 prepared with 1.5 g of PS template yielded a product with an irregular morphology (**Figure S13**) and almost no crystalline phase. The mercury intrusion curves (**Figure S13e**) reach a saturation of 0.29, 0.47, 0.54 $\text{mL}_{\text{Hg}}/\text{g}$ for the C-NTU-9, Hier-NTU-9-S1, and Hier-NTU-9-S2, respectively, indicating that more PS templates yield a product with more macropores that can provide more space for bulky materials. The macropore size of the resultant Hier-NTU-9-S2 is also in the range of 100-1000 nm (**Figure S13f**), giving a larger macropore area of $510 \text{ m}^2/\text{g}$ than that ($250 \text{ m}^2/\text{g}$) of the Hier-NTU-9-S1 (**Table S1**).

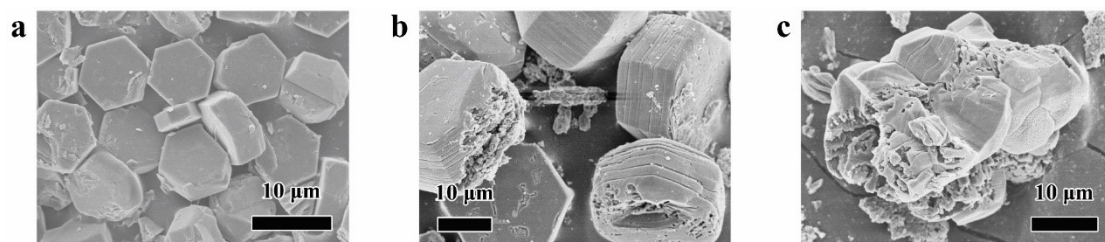


Fig. S14 SEM images showing the morphology of used catalysts. (a) C-NTU9, (b) Hier-NTU-9-S1, and (c) Hier-NTU-9-S2.

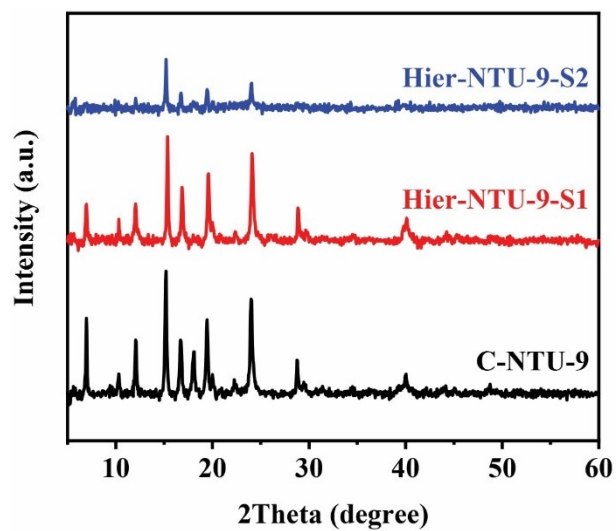


Fig. S15 XRD patterns of used catalysts.

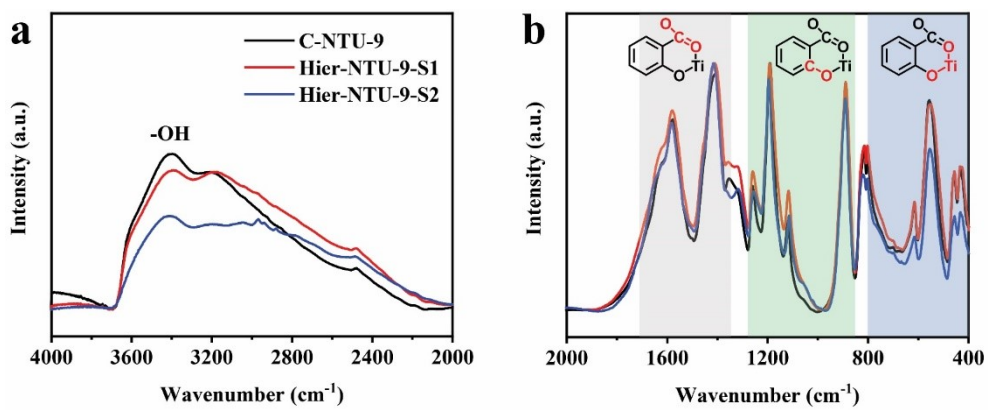


Fig. S16 IR spectra ranging from 2000-4000 cm^{-1} or 400-2000 cm^{-1} of used catalysts.

Table S1. Macropore properties of samples determined by mercury intrusion porosimetry.

	S_{Macro} (cm^2/g)	<i>Intrusion</i> (mL/g)	<i>Porosity</i> (%)
C-NTU-9	0	0.29	15.73
Hier-NTU-9-S1	260	0.47	19.14
Hier-NTU-9-S2	510	0.54	20.71

Table S2. Textural properties of samples.

	S_{BET} (m^2/g)	S_{micro} (m^2/g)	S_{exter} (m^2/g)	V_{total} (cm^3/g)	V_{micro} (cm^3/g)	V_{exter} (cm^3/g)
C-NTU-9	722	595	127	0.45	0.33	0.12
Hier-NTU-9-S1	855	556	299	0.50	0.31	0.19
Hier-NTU-9-S2	387	306	81	0.29	0.17	0.12

Surface area (S) and pore volume (V) were determined by N_2 adsorption-desorption

Table S3. Catalytic performance of ODS reactions of different reactants over microporous or Hierarchically porous NTU-9 catalysts.

	BT (%)		DBT (%)		DMDBT (%)	
	1st cycle	3th cycle	1st cycle	3th cycle	1st cycle	3th cycle
C-NTU-9	19.27	19.69	47.53	47.30	33.30	33.73
Hier-NTU-9-S1	35.82	36.76	75.89	75.75	76.84	75.98
Hier-NTU-9-S2	27.75	/	68.18	/	56.50	/
S3	4.65	/	4.06	/	3.68	/

Reference

- 1 K. Shen, L. Zhang, X. Chen, L. Liu, D. Zhang, Y. Han, J. Chen, J. Long, R. Luque, Y. Li and B. Chen, *Science*, 2018, **359**, 206–210.
- 2 M.-H. Sun, J. Zhou, Z.-Y. Hu, L.-H. Chen, L.-Y. Li, Y.-D. Wang, Z.-K. Xie, S. Turner, G. Van Tendeloo, T. Hasan and B.-L. Su, *Matter*, 2020, **3**, 1226–1245.
- 3 H. Chun and D. Moon, *Cryst. Growth Des.*, 2017, **17**, 2140–2146.